Novel Approach on Sparkle Contrast Measurement by utilizing Diffraction Blur

Makio Kurashige, Gen Furui, Shumpei Nishio, Kazutoshi Ishida, Mitsuhiro Kuzuhara, Hiroko Suzuki, Jun Tsujimoto, Masayuki Tsunekawa, Yukimitsu Iwata, Norinaga Nakamura

kurashige-m@mail.dnp.co.jp
Dai Nippon Printing Co., Ltd., 250-1, Wakashiba, Kashiwa, Chiba, 277-0871, Japan
Keywords: sparkle, sparkle contrast, anti-glare display

ABSTRACT

The conditions of sparkle contrast measurement which were not affected by the modulation of display matrix image itself were investigated in the viewpoint of optical imaging. The proposed method utilizing diffraction blur by the circular aperture of imaging lens enabled to get accurate, reproducible, comparable data within the proposed conditions.

1. INTRODUCTION

Sparkle effect derived from Anti-Glare Layer (AGL) on the displays are well known. Several measurement methods have been proposed to characterize this phenomenon [1], [2]. Sparkle was observed as a spatially modulated image on the retina, which was a result of imaging a display matrix through AGL. Sparkle level was characterized by the sparkle contrast S_P which was defined as a formula (1),

$$S_{\mathrm{P}} = \frac{\sigma}{\bar{I}} \quad (1)$$

where σ was the intensity standard deviation of the sparkle pattern, $\bar{I}$ was the average of it. S_P was dependent on various parameters. In terms of optical imaging, it was reported that the aperture angle and effective imaging F-number: $F\#_{image}$ shall be same to compare the measured S_P [3]. In case that the image of display matrix itself was overlapped on the sparkle pattern, post-processing filters have been used to separate the periodic modulation derived by the display matrix. These filtering methods were for the "oversampling" conditions, which Image Sampling Ratio (*ISR*) was over 1. *ISR* was defined as a formula (2),

$$ISR = \frac{mP_{\mathrm{F}}}{P_{\mathrm{L}}} = \frac{P_{\mathrm{D}}}{P_{\mathrm{L}}} \quad (2)$$

where P_F was a fundamental pitch of display subpixels, m was optical magnification, P_D was a fundamental pitch of the image of the display subpixels, P_L was a pitch of LMD (Light Measuring Device) pixels. However, the properties of each filter make it difficult to compare the measured sparkle contrast mutually. For example, in case of Moving Window Averaging (MWA) filter [2], random components of the sparkle pattern were also affected by the filtering process. It was difficult to get comparable data among the different filter design, i.e. different measurement setup or LMDs (generally, MWA filter has been used for the fixed display matrix design with the fixed measurement configurations to compare the performance of AGL components). Other example was a notch filter in frequency domain [4]. Indeed, this method enabled only to remove periodic components while preserving the random components as original as possible. But in general, this filter would include engineering knowhow, which could not be specified perfectly. Therefore, it might not be widely applied to all the cases, even if a skilled engineer could get accurate and reproducible results. In addition, moiré which depends on *ISR* would affect the results for both filters. On the other hand, in case of undersampling, i.e. *ISR* under 1, original image of display matrix could not be measured because of the sampling theory. There was no filter directly applied in this case, but the possibility of generating moiré was reported [5]. Actually, the measurement error was confirmed in the lower $F\#_{image}$ [3], although the source of generating moiré could not be specified directly. With considering these situations, it was necessary to specify the imaging conditions which could be universally used and were not affected by moiré regardless of *ISR*.

2. Simulation

2.1. Moiré effect by imaging display matrix

The simulation of the imaging process was conducted with assuming the parameters in Table 1. The lens focus was supposed to be on the display matrix.

Table 1. Parameters for simulation.

Focal length of the imaging lens: f_∞ (Effective focal length: f)	50 mm (54.4 mm)
Measurement distance: L	620 mm
Fundamental pitch of the display subpixel : P_F	60 μm
Optical magnification: m	0.0877
Effective imaging F-number: $F\#_{image}$	4.35 ~ 17.4
Pitch of the imaging sensor array : P_L	1.2 μm ~ 9.0 μm

Fig.1 was a model of the imaging process of display matrix. Fig.1 (a) was virtual modulation of the image of display matrix with 10 cycles of display subpixel on the LMD sensor only considering the optical magnification. The display was assumed to be operated full-screen uniform green, equipped with a colour filter of simple

RGB stripe (i.e. the fill factor of G subpixel was set at 30%). Optical image would be affected by the diffraction of lens iris. Fig.1(b) showed a Point Spread Function (PSF) at the diffraction limit, i.e. Airy disc on the LMD sensor, in case $F\#_{image}$ was 4.35 at a wavelength of 530 nm. For the simplicity, only the part inside the first minimum of the Airy disc was considered. Fig.1 (c) was a result of simulating the optical image on the LMD sensor by the convolution of Fig.1 (b) over Fig.1 (a). Finally, Fig.1 (d) showed the results of sampling the modulation in the Fig.1 (c) with P_L of 3.8 μm, i.e. *ISR* = 1.38. The moiré pattern with the broader pitch compared to the Fig.1 (c) was obtained.

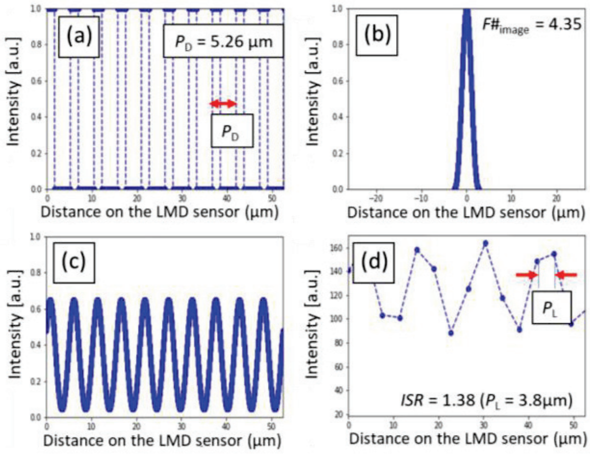

Fig.1. Imaging procedure of the display matrix with considering the diffraction blur.

For details of the moiré pattern, the effect of P_L was investigated by using same optical modulation in the Fig.1 (c). The simulated results by the different P_L from 1.2 μm to 9.0 μm were shown in Fig.2. Various frequencies and intensity variations of the moiré patterns were generated even if the original optical modulation was same.

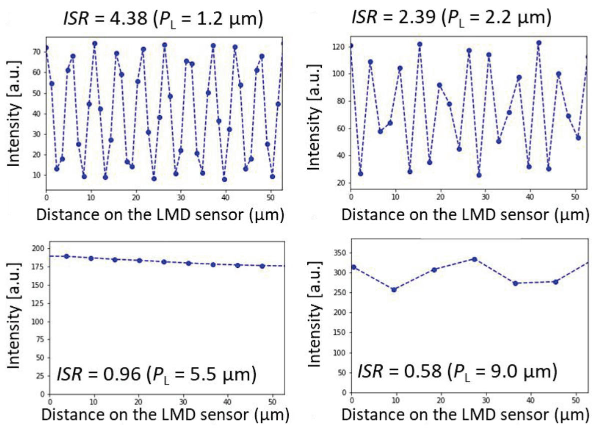

Fig.2. Simulated moiré patterns with various P_L.

In case of oversampling conditions, post-process filter can be used to separate the fundamental periodic components of the display matrix image, although the results could only be comparable within the same filter design. The simulated results by applying MWA filters with several P_L were shown in Fig. 3. The original modulation was same as the Fig.1 (c). When *ISR* was integer, there was no moiré pattern. However, in other cases, moiré patterns still existed although the fractional kernel [2] of MWA filters were applied.

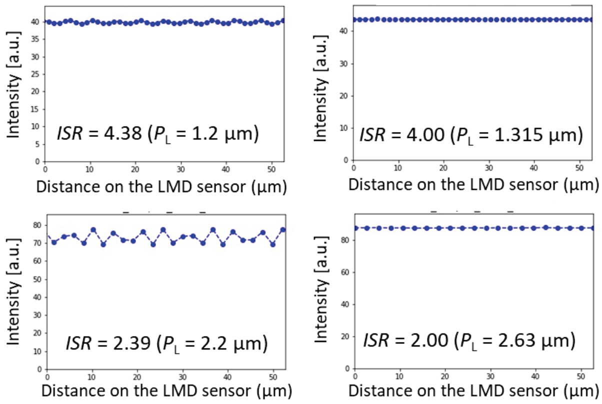

Fig.3. Simulated moiré patterns with various P_L after applying MWA filter.

2.2. Imaging conditions to suppress the moiré pattern by utilizing diffraction blur

The frequency and the intensity variation of the moiré pattern would be easily changed if one of the parameters in the Table 1 varied. This was a potential risk of measurement error even if AGL on the display matrix would disturb the original modulation of the display matrix to some extent. Therefore, it was necessary to find out imaging conditions which the moiré pattern was suppressed enough through the wide range of *ISR*. The idea for this solution was to achieve uniform intensity distribution at the stage of the Fig.1 (c), since no moiré pattern would be generated if there was no optical modulation on the LMD sensor. This could be achieved when the diameter of PSF at the Fig.1(b) was wider enough than P_D. The diameter of the first minimum of Airy disc *A* was written as a formula (3)

$$A = 2.44 F\#_{image} \lambda \tag{3}$$

where, λ was wavelength. λ would have certain range even if the displayed colour was single colour of subpixel. In that case, dominant wavelength could be used for this purpose.

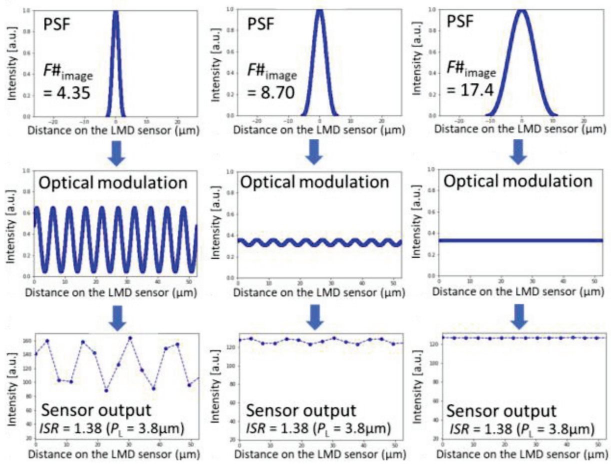

Fig.4. Simulated results by different $F\#_{image}$

The simulated results with different $F\#_{image}$ were shown in Fig.4. With increasing $F\#_{image}$, the optical modulation became uniform, and the modulation of the moiré pattern from the sensor output was disappeared. To figure out the boundary of $F\#_{image}$ which the optical modulation became uniform, the coefficient of variation C_V and the evaluation parameter R_D were introduced in formula (4) and (5),

$$C_V = \frac{\sigma_V}{\bar{I}_V} \tag{4}$$

$$R_D = \frac{A}{P_D} \tag{5}$$

where σ_V was the standard deviation of the sensor output, $\bar{I}_V$ was the average of it. Fig. 5 showed the simulated results when $F\#_{image}$ was changed from 4.35 to 17.0 by the different P_L. In all the cases, C_V was getting close to zero around R_D of 3, although huge difference was measured in the smaller R_D region.

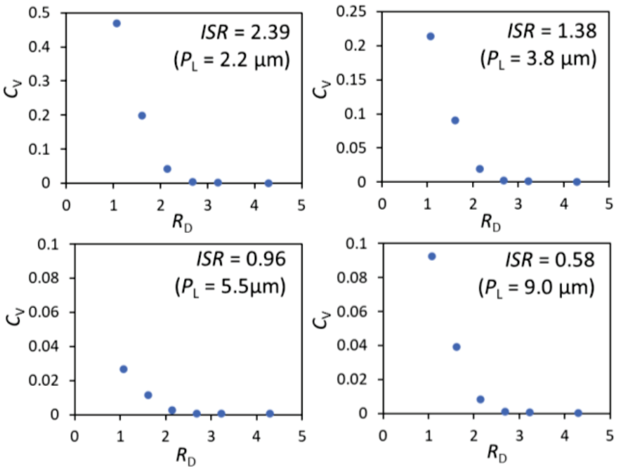

Fig.5. Relation of C_V and R_D (Simulation).

Thus the requirement for the imaging condition to avoid moiré effect could be written as a condition (6),

$$R_D \geq 3 \tag{6}$$

With using the formula (3) and (5), the condition (6) was also expressed as

$$\frac{F\#_{image}\lambda}{P_D} \geq \frac{3}{2.44} \cong 1.25 \tag{7}$$

This condition would be conservative because it was assumed that the imaging lens was free of aberration with the best focusing.

3. EXPERIMENTS

3.1. Measurement conditions and procedure

The measurement configuration of sparkle contrast was shown in Fig.6.

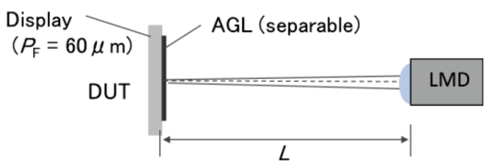

Fig.6. Setup for sparkle measurement.

The imaging LMD was set in front of the display equipped with AGL from the measurement direction normal to the display. The lens focus of the LMD was set on the display matrix. Image was captured by CCD camera. The other parameters were described in each following sub-section.

3.2. Comparison of measured moiré patterns with the simulated results

For the measurement of reproducing the moiré patterns simulated in the section 2, the AGL was tentatively removed from the DUT. The measurement conditions were listed in Table 2.

Table 2. Measurement parameters in 3.2.

f_∞ (f)	50 mm (54.4 mm)
L	620 mm
$F\#_{image}$	4.35
P_L	3.75 μm, 5.5 μm, 9.0 μm

The results were shown in Fig. 7. The frequency of the moiré patterns were similar between the simulation and the measured data. The number of subpixel of the display matrix had been varied from 10 to 100 for the easy observation of the moiré patterns. The deviations were observed in terms of amplitude, i.e. slightly larger (*ISR* = 0.96), smaller (*ISR* = 0.58), or similar (*ISR* = 1.40). This might be caused by the detector aperture of the LMD pixel. In the simulation, the whole area of each pixel was assumed as uniform detector. However, in general the detector aperture would be smaller than the pixel, and be different by each product design of the sensor.

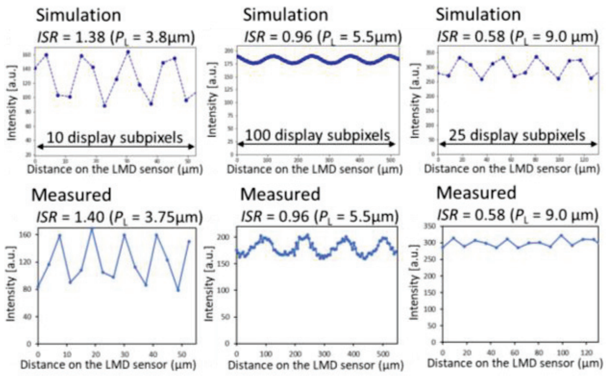

Fig.7. Comparison of the moiré pattern between the simulation and the measured data (*F#* =4.35).

The relation of C_V and R_D was also checked as shown in Fig.8. As simulated in the Fig. 5, C_V was suppressed over R_D of 3.

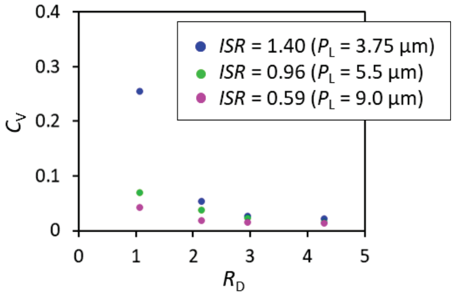

Fig.8. Relation of C_V and R_D (measured).

3.3. Sparkle contrast measurement not affected by moiré patterns

Under the condition (7), the modulation of the optical image of the display matrix was suppressed by the enough diffraction blur on the LMD sensor, i.e. only the random components of the sparkle pattern could be obtained. The measured sparkle contrast would be same when the resolution spot of the LMD on the display surface *S* and $F\#_{\text{image}}$ in the formula (8) and P_L were fixed [3],

$$S \propto \frac{F\#_{\text{image}}}{m} = F\#_{\text{image}} \frac{L}{f} \qquad (8).$$

When P_F and *m* were same as in the Table 2, the condition (7) was $F\#_{\text{image}} \geq 12$ at λ=530nm. For the measurement with P_L of 9.0 μm, *L* and *f* were chosen to keep same *m* as listed in Table 3.

Table 3. The conditions of *f* and *L* under the same *m*.

f_∞ (*f*)	*L*
50 mm (54.4 mm)	620 mm
60 mm (65.3 mm)	745 mm
85 mm (92.4 mm)	1055 mm
105 mm (114.2 mm)	1300 mm

The measured sparkle contrast under different $F\#_{\text{image}}$ was shown in Fig.9. As theoretically derived in [3], the same sparkle contrast was obtained at the same $F\#_{\text{image}}$ among the different conditions.

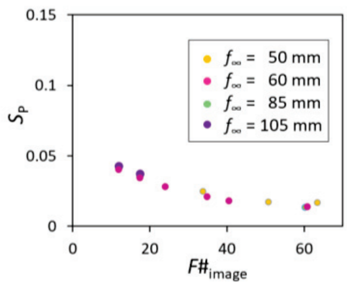

Fig.9. Sparkle contrast by optically equivalent conditions with satisfying the condition (7).

The last example was the case of comparing the sparkle contrast obtained by the different P_L. The integration effect of the sparkle pattern on the LMD pixels could be occurred [3]. The measured sparkle contrast would be lower than the one which was expected by the actual optical modulation. The degree of integration depended on P_L. However, if only the random components of the sparkle pattern were measured, the sparkle contrast before the integration could be restored by cancelling the integration effect with mathematical operation. The sparkle contrast, which only the integration effect was considered, was expressed as a formula (9) with an integration factor *M*,

$$S_P = \sqrt{\frac{1}{M}} \qquad (9)$$

M was represented by using P_L and $F\#_{\text{image}}$ as a formula (10),

$$M = \left[\sqrt{\frac{4}{\pi}} \frac{F\#_{\text{image}}\lambda}{P_L} \operatorname{erf}\left(\frac{\pi P_L}{2F\#_{\text{image}}\lambda}\right) - \left(\frac{2F\#_{\text{image}}\lambda}{\pi P_L}\right)^2 \left\{1 - \exp\left(-\left(\frac{\pi P_L}{2F\#_{\text{image}}\lambda}\right)^2\right)\right\} \right]^{-2} \qquad (10)$$

where erf was a standard error function. The restored sparkle contrast $S_{P\text{-}R}$ from the measured one was obtained by the formula (11),

$$S_{P\text{-}R} = \sqrt{M} S_P \qquad (11)$$

The measurement conditions were listed in Table 4.

Table 4. Measurement parameters to obtain S_P.

f_∞ (*f*)	50 mm (57.1 mm)
L	400 mm
P_L	6.45 μm, 9.0 μm

The condition (7) was $F\#_{\text{image}} \geq 19.5$ at λ = 530nm. The measured results of both S_P and $S_{P\text{-}R}$ were shown in Fig. 10. In the Fig.10 (a), small deviation was observed around the $F\#_{\text{image}}$ of 20 although the results were almost in the same line at the higher $F\#_{\text{image}}$. This was a phenomenon along with the theory, which the integration effect was rapidly getting stronger in the lower $F\#_{\text{image}}$. In the Fig.10 (b), both data became quite similar by cancelling the integration effect.

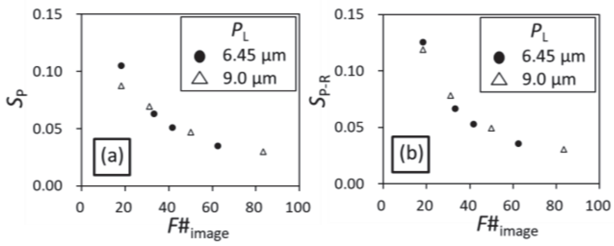

Fig.10. Measured sparkle contrast (a) and restored sparkle contrast (b) with satisfying the condition (7).

4. CONCLUSIONS

The generation mechanism and the variety of the moiré pattern when imaging the display matrix were analyzed by the simulation. The universal imaging conditions which were not affected by the moiré pattern were validated by the experiments. The proposed method could be applied through the whole range of *ISR* without post-processing filter to remove the periodic modulation derived from the display matrix structure.

REFERENCES

[1] G. Furui, US patent no. US6697515B2 (2003).

[2] M. E. Becker and J. Neumeier, “Optical Characterization of Scattering Anti-Glare Layers”, SID Symposium Digest 42, 1038-1041 (2011).

[3] M. Kurashige et al, “Estimation of Equivalent Conditions for Display Sparkle Measurement”, Proc. IDW19, VHF1-3 (2019).

[4] M. Kurashige et al, “Sparkle Measurement of Anti-Glare Displays with Simulating Human-Eye Perception”, Proc. IDW18, VHF4-3 (2018).

[5] M. Isshiki et al., “The Optimized Condition for Display Sparkle Contrast Measurement of Anti - Glare Cover Glass based on the Solid Understandings”, SID Symposium Digest 50, 1126-1129 (2019).